Pannu *J Wireless Com Network* (2024) 2024:48
https://doi.org/10.1186/s13638-024-02369-1

EURASIP Journal on Wireless Communications and Networking

RESEARCH Open Access

Highly compact UWB-MIMO antenna with sharp multi-stop band characteristics

Preeti Pannu[1*]

*Correspondence:
preetipannu7@gmail.com

[1] Department of ECE, Guru Nanak Dev Engineering College, Ludhiana, Punjab, India

Abstract

With multi-band rejection characteristics, a new low-profile antenna of size 34 × 34 mm2 is conferred in this article. It consists of quad identical monopole elements (originated orthogonally), contributing ultra-wideband characteristics in the system. The single unit of the proposed design consists of a modified spinning-top shape radiator (MSTSR), excited by a tapered microstrip line feed (TMLF) and semi-circular ground. An excellent bandwidth of 3–12.9 GHz (where S11 < − 10 dB) is obtained at each port. By inserting the structure of four spiral coils, a sharp notch ranging from 7.9 to 8.5 GHz is achieved to filter the X-band satellite communication uplink. In addition, a circular spiral slot in the radiator near the ground plane creates a stop band at 7.35–7.565 GHz band (satellite communication downlink band). Furthermore, symmetrical rectangular trapezoid resonators and inverted symmetrical rectangular trapezoid structures near the feed line are responsible for the elimination of interferences at 5.5 GHz lower WLAN and 3.5 GHz WiMAX respectively. The FR-4 substrate used for the UWB-MIMO design fabrication process and fabricated results are found in good match with the simulated results. Also, the design provides good performance metrics such as total active reflection coefficient, diversity gain, channel capacity loss, isolation, and envelope correlation coefficient.

Keywords: MIMO, UWB, Notched band, Diversity, MSTSR, TMFL

1 Introduction

The modernization in wireless and mobile technologies demands efficient antenna modules that have compact size, easy fabrication, high radiation efficiency, high data-rate capacity, large bandwidth, and low power requirement [1–28, 23–28. The efficacy of well-known Ultra-wideband antennas makes them an attractive choice in recent years. In the year 2002, ultra-wideband communication got an unlicensed spectrum ranging from 3.1 to 10.6 GHz from the Federal Communication Commission (FCC) 4. Due to the wide spectrum of such antennas, their effective deployment has been seen in many applications such as tracking and navigation systems, cognitive radios, spread-spectrum communication, wireless sensor networks, military applications, and soon 5, 6. The performance of UWB systems is limited by fading problems which occur because of various phenomena such as reflection, refraction, and diffraction of electromagnetic waves. Multipath fading degrades the transmission quality of signal in free space. To combat

its effect, various diversity/MIMO techniques have been reported in the literature. The multiple input multiple output (MIMO) approach is highly suitable for reducing fading effects thereby attaining high data rates, range, robust, secure, and reliable communication. In addition, by combining UWB technology and the MIMO approach, the system throughput and transmission power can be improved.

The design of a compact UWB system with multiple antennas is a challenging task due to space constraints. The closely operating frequencies and space issues result in strong mutual coupling among the antenna elements. The isolation among multiple radiating elements in a system can be enhanced by adopting various decoupling structures including various slits, decoupling strips, different shaped stubs; orthogonal orientation of antenna elements; providing spacing between radiating elements; using the slotted-edge-substrate method, and soon [7–22. However, various decoupling structures occupy more space, and make the antenna configuration much complex [7–9. It has been observed that antenna size increases with greater spacing between radiating elements. Consequently, compactness in antenna size, design complexity minimization, and coupling minimization are the main concerns in MIMO design for UWB communication.

The overlap of existing licensed bands such as WLAN, WiMAX, etc. with that of Ultra-wideband results in the overlapping of electromagnetic signals. This electromagnetic interference is another challenge faced by UWB antennas. The remedy for this is to design an antenna with a notch behavior. Many UWB-MIMO systems with notch behavior have been developed in recent years. A UWB-MIMO antenna with single-notch behavior has been reported in 10, where L-shaped slits have been used to create a notch at the WLAN band. A dual-port MIMO antenna with arc-shaped slot resonators in CPW feed for stop-band is presented. In reference 12, a pair of inverted L-strips is used to provide dual notches at bands ranging from 5.15–5.85 and 6.7–7.1 GHz. UWB-MIMO antenna integrated with EBG structures to attain three stop-bands at Wi-MAX, WLAN, and X band reported in reference 13. A compact MIMO with band notch at WLAN and good isolation has been reported in.14 UWB-MIMO antenna designs with decoupling resonators 15, parasitic decoupling structure attached to ground plane 16 and ground stubs 17 has reported with very low coupling. A 4×4 UWB-MIMO design consists of slotted circular disc-shaped radiators with dual notches reported in reference 18, where large spacing is used for improving isolation among antenna elements which in turn increases the design size to 81×87 mm^2. In reference 19, a quad-port MIMO with dual-band notches using complementary split ring resonators and good diversity by slotting substrate was presented. A Koch fractal MIMO design with grounded stubs for isolation and a C-shaped slotted radiator for notch characteristics was reported 20. A UWB antenna with an LC band stop filter and good isolation is presented in reference 21. A MIMO antenna with a quasi-self-complimentary structure contributes to wide band characteristics as well as additional decoupling presented in 22, in which a notched band is obtained using a bent slit in the patch.

2 Methods/experiment

Among the existing designs of notched-band UWB-MIMO antenna as discussed in the previous section, it is difficult to maintain the compactness, low coupling levels, the center frequency of notches, and sharpness of notch-bands. Moreover, most of the

reported designs have either one, two, or three notches at maximum. So, it is required to design a simple, small, and efficient MIMO system with low coupling issues, high isolation, easy fabrication, and a large number of unwanted frequency suppression to stop interference through numerous existing bands. In this article, a novel 4-port UWB MIMO antenna on FR-4 substrate is presented with sharp multiple-band notched behavior (very few in existing literature). The design consists of identical four modified spinning-top shape radiators (MSTSR) which are orthogonally placed to provide polarization diversity. In this way, inter-element isolation amongst the four ports is improved. The four radiators fed through taper-off microstrip lines, contributing to ultra-wideband characteristics. In the design structure, Notching at the X-band satellite communication uplink (Notch#1) is achieved by inserting four spiral coils on the side of the semi-circular ground plane. Notch#2 is obtained by etching a circular spiral slot inside the MMSR covering the X-band satellite communication downlink. The presented design is very effectively utilizing the spectrum, eliminating the interference from existing bands and supporting various wireless applications. Furthermore, by inserting symmetrical trapezoid rectangular resonators and inverted symmetrical trapezoid rectangular resonators on either side of radiators, notch#3 is obtained at 5.5 GHz covering WLAN and notch#4 is obtained at 3.5 GHz covering WiMAX band respectively. A detailed description of the proposed prototype is presented in the preceding sections. The CST studio simulation software was used for designing the prototype. Table 1 shows a comparison analysis of the designed antenna with the other reported UWB designs in the literature. The designed antenna is advantageous over reported designs in terms of (1) Relatively small in size(34×34mm2); (2) More monopoles enhance the system throughput and transmission capacity; (3) Multiple stop band property; (4) Stop bands are simply obtained by utilizing simple structures and slot without any significant compromise with size, isolation factor, complexity, and radiation performance; (5) The center frequencies of stop bands are relatively sharp; (6) the notches has a relatively narrow band; (7) Inter-monopole isolation is relatively high without using any complex decoupling structures; (8) Almost all MIMO performance parameters are evaluated; (9) Proposed UWB MIMO with multiple notches design is rare in the existing literature.

3 Antenna design

3.1 Design of unit modified conical shape radiator

The geometrical details of proposed unit element and ground plane are given in Fig. 1a, b respectively. The dimension of unit cell is $16 \times 18 \times 1.6$ mm^3. The layout is presented using a cheap FR4 substrate of thickness 1.6 mm. The monopole antenna consists of micro strip line fed modified spinning-top shape radiator. The feed-line is tapered off in a balanced manner in order to obtain the UWB characteristics. The parametric particulars of antenna are listed in Table 2.

Beneath the radiator, a structure of four spiral coils is inserted above the ground plane to notch the uplink band of satellite communication. The details of the structure are illustrated in Fig. 1c. For achieving notch band characteristics at satellite communication downlink, a spiral slot is embedded in the MSTSR. By controlling the length of the spiral slot, the bandwidth of the notch is controlled. Further, notching at 5.5 GHz and 3.5 GHz respectively is obtained by inserting a pair of rectangular trapezoidal structures(structure

Table 1 Comparison of proposed design with other literature antennas

Refs.	No. of elements	Size (in mm^3)	Bandwidth (in GHz)	Notch bands (in GHz)	ECC	TARC (in dB)	Channel capacity (in bits/s/Hz)	DG (in dB)	Isolation (in dB)
[5]	1	12 × 19x1.6	2.95–12	3.3–3.8, 5.1–5.825, 7.25–7.75	–	–	–	–	–
[6]	1	20 × 40x0.762	3.1–10.5	5.725–5.85, 8.025–8.4	–	–	–	–	–
[7]	2	22 × 31x0.125	3–10	–	< 0.3	–	< 0.4	–	> 15
[8]	2	32 × 32x0.8	3.1–10.6	–	< 0.04	–	–	–	> 15
[9]	2	25 × 45x0.8	3.1–12	–	< 0.2	–	–	> 9.5	> 15
[10]	2	38.5 × 38.5x1.6	3.08–11.8	5.03–5.97	< 0.02	–	–	-	> 15
[11]	2	50 × 50x1.524	2.8–10.8	4.75–6.12	< 0.02	–	–	–	> 15
[12]	2	26 × 28x0.8	2.9–10.8	5.05–5.86, 6.68–7.43	< 0.08	< -12		> 9.95	> 15
[13]	2	64 × 45x1.6	2.5–11	3.3 to 3.6, 5 to 6, 7.1 to 7.9	< 0.02	–	–	–	> 15
[14]	2	30 × 30 × 1.6	3.1–11	4.98–5.96	< 0.02	< -10	< 0.35	9.51	> 20
[15]	4	40 × 40x1.6	3.1–11	–	< 0.004	–	< 0.4	-	> 20
[16]	4	40 × 43x1	3.1–10.6	–	< 0.2	-8	< 0.3	-	> 20
[17]	4	35 × 35 × 0.8	3–12	–	< 0.07	–	–	–	> 15
[18]	4	87 × 81x1.6	3.03–10.74	3.87–5.94, 7.04–8.7	< 0.1	–	–	–	> 20
[19]	4	58 × 58x0.8	3–13.5	3.25–3.75, 5.3–5.7	< 0.008	–	–	> 9.9	> 22
[20]	4	45 × 45x1.6	2–10.6	5.15–5.85	< 0.003	–	< 0.1	-	> 17
[21]	4	50 × 39.8x1.524	2.7–12	5.1–5.9	< 0.03	–	–	–	> 17
[22]	4	35 × 35x1	3–12	5.15- 5.825	< 0.5	–	–	–	> 20
Prop. Work	4	34 × 34x1.6	3–12.9	7.9–8.49, 7.36–7.72, 5.3–5.61, 3.4–3.66	< 0.016	< -6 except at notch bands	< 0.1	> 9.92	> 17

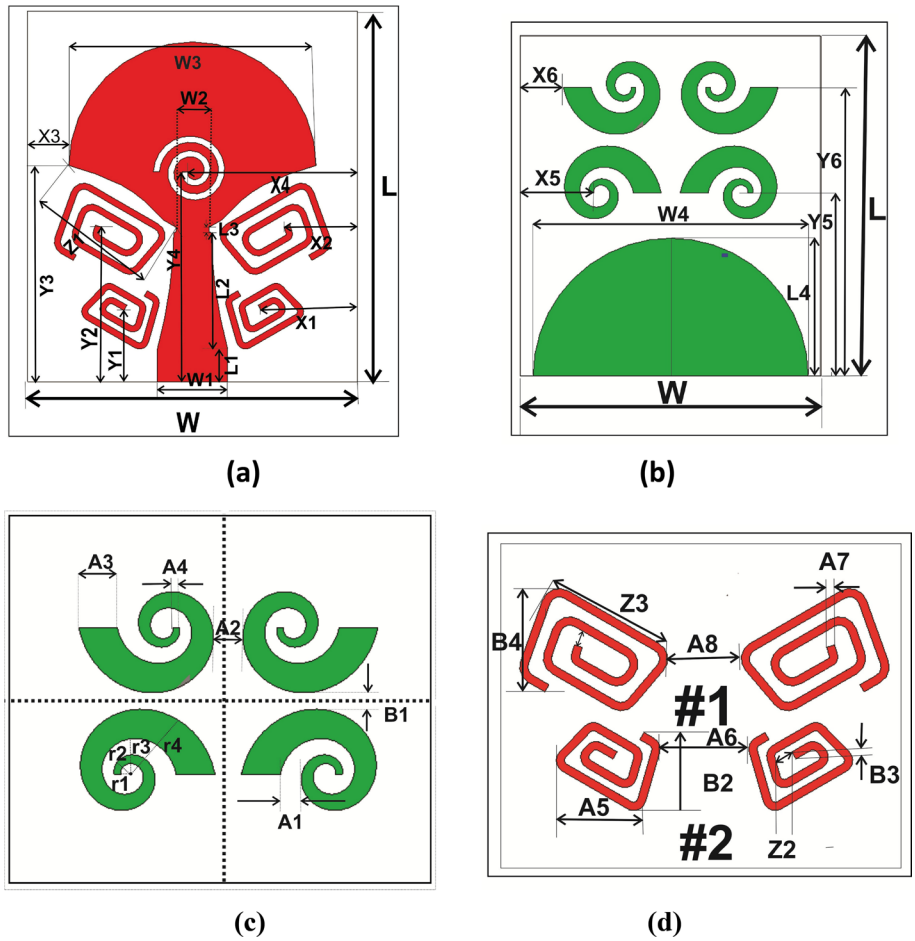

Fig. 1 Shows the Monopole antenna geometry **a** Unit cell Radiator **b** Ground plane **c** Spiral coil structure **d** Trapezoidal Structure #1 and #2

#2) and a pair of inverted rectangular trapezoidal structures(structure #1) symmetrically near the feed line. The detail related to the dimensions of structures is provided in Fig. 1d. The CST Microwave Studio platform is used for various designing steps, simulations, and optimization processes. The design steps of the proposed monopole are represented in Fig. 2. The simulated S-parameters for the seven evolutional prototypes are shown in Fig. 3. A spinning-top shape radiator with a semi-circular ground plane, fed through a 50Ω rectangular microstrip line is designed in Fig. 2a. It possesses narrow bandwidth of 10–12 GHz. In step 2, the rectangular feed line is tapered (TMFL) which improves the port reflection characteristics. This step gives high eccentricity to support multiple modes, required for UWB operation. But, in the 6–8 GHz frequency range, it has a bad reflection coefficient graph. Further, to improve the reflection coefficient characteristics in the middle-frequency band, the lower edges of the mushroom shape radiator are tapered asymmetrically (step 3).

The TMFL is also optimized for 50Ω impedance matching with the radiator to reduce the reflection of incident waves. This Modified Spinning-top shaped radiator (MSTSR) with TMFL provides the necessary balanced impedance and enhances the current path. A tapered conducting patch (MSTSR) maintains good impedance bandwidth

Table 2 Optimized Designing Parameters for Proposed antenna

Dim	Val. (in mm)	Dim	Val. (in mm)
L	18	Y6	15.25
W	16	A1	0.77
W1	3.4	A2	1.23
W2	1.6	A3	1.37
W3	12	A4	0.26
W4	14.6	A5	3.6
L1	1.6	A6	3.65
L2	5.68	A7	0.3
L3	0.3	A8	2.67
L4	7.3	B1	0.68
X1	4.62	B2	2.84
Y1	3.57	B3	0.3
X2	3.5	B4	4.5
Y2	7.53	r1	0.44
X3	2	r2	0.71
Y3	10.5	r3	1.28
X4	7.81	r4	2.44
Y4	10	Z1	6
X5	4	Z2	0.65
Y5	9.75	Z3	5.08
X6	2.4		

throughout the UWB. To realize the desired notches in the UWB spectrum, antenna design needs to be further modified. Multiple resonance structures may be provided for suppressing multiple bands. The various notch structures do not need to be on the same side of the monopole. In step 4, four capacitively coupled spiral coils are used behind the radiator to produce additional resonance to suppress the desired band. The length and position of the structure are selected to entirely cover the radiator linked with the stop band and therefore determine the bandwidth that is to be suppressed. Two degrees of freedom in defining the location and shape (including width and length) of the resonant structure can be used to control the notch frequency range. This four-spiral structure creates a notch in the bandwidth of 8–8.67 GHz (notch#1). Also, the upper two spirals of the 4-spiral structure are responsible for poor return loss in the 7.86–7.96 band.

In step 6, tri-band notch characteristics are achieved by further modifying the structure. To create notch #3 in the 5.29–5.68 GHz band, two rectangular trapezoid resonators are inserted close to the feed line's bottom edge. The length of the trapezoids is optimized to get the desired stop band. The position of trapezoids is near the feed line so that current in the feed line affects and a notch at a desired frequency can be created. These resonators also cause changes in notch #1 and notch #2 frequency bands to the 8.25–8.59 GHz band and 7.61–7.93 GHz band respectively. The changes in notch occur due to the coupling effect of introduced structures. Further, symmetric inverted rectangular trapezoid resonators are inserted near the upper edge of the feed-line responsible for notch #4 at the 3.4–3.79 GHz band. This notch having a central frequency of 3.5 GHz covers the WIMAX band. The fourth notch creates a change in the previous three notch frequency bands due to the coupling effects of the modified design. Now, Notch #1

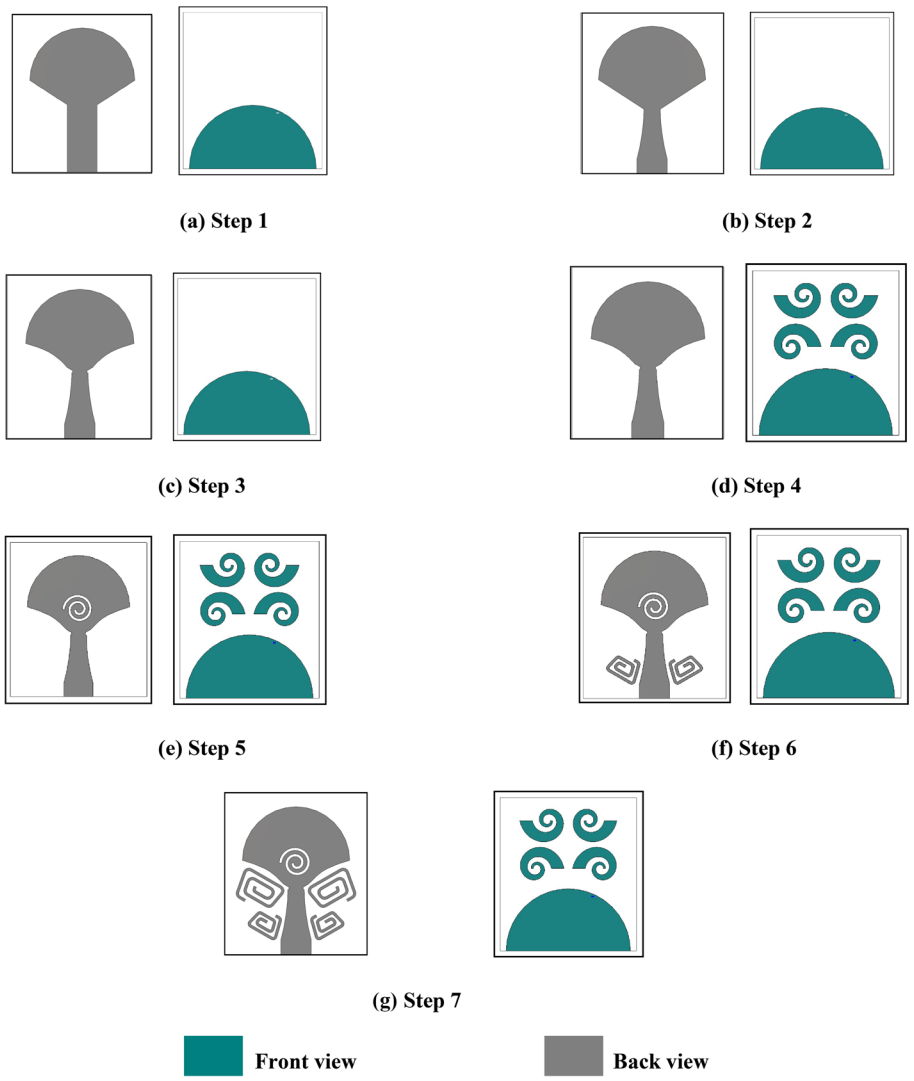

Fig. 2 Shows evolution steps of proposed UWB Monopole antenna

covers the satellite communication uplink band from 8.07 to 8.72 GHz and Notch #2 covers the satellite communication downlink band from 7.39 to 7.90 GHz band. Lastly, Notch #3 covers the WLAN band from 5.31–5.75 GHz band.

3.2 Design of 2-port MMSR MIMO

The layout for the MIMO design with two monopoles is shown in Fig. 4a. The dimensions of the antenna are 17×34 mm^2. A 2-monopole design is presented by the orthogonal orientation of monopoles. This reduces the coupling effect among the antenna elements. The S21 plot represents that the isolation factor of more than 20 dB has been achieved throughout the spectrum. Figure 4b shows simulated reflection coefficients of the two-port design, highlighting the UWB performance and quad-band elimination characteristics. The simulated impedance bandwidth for two port MIMO antenna ranges from 3.064 to 12.92 GHz with stop bands from 3.41 to 3.79 GHz, 5.32–5.55 GHz, 7.36–7.69 GHz, and 7.85–8.5 GHz. The notches obtained are sharp and narrow. The

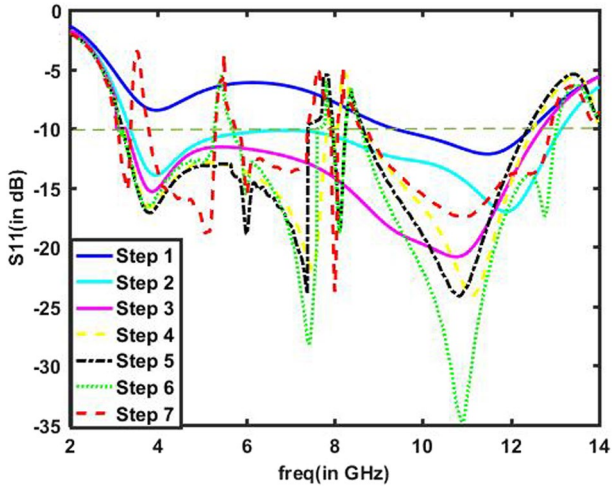

Fig. 3 Shows S-parameters for various design steps

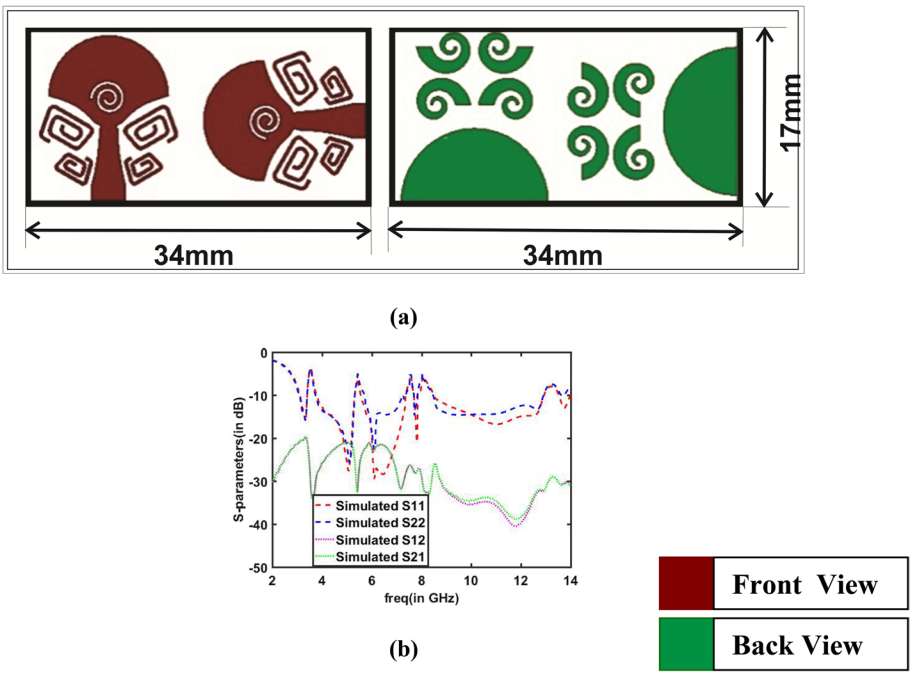

Fig. 4 Shows dual monopole MIMO design **a** Geometric layout **b** Simulated S-parameters

MIMO performance parameters Envelop Correlation Coefficient, Diversity Gain, and Total Active Reflection Coefficient are evaluated. ECC among monopole elements can be evaluated by the relation

$$\mathbf{ECC}(1,2,2) = \frac{\left|S_{11}^{*}S_{12} + S_{21}^{*}S_{22}\right|^{2}}{\left(1-|S_{11}|^{2}-|S_{21}|^{2}\right)\left(1-|S_{22}|^{2}-|S_{12}|^{2}\right)} \tag{1}$$

where, $i=1, j=2, N=2$.

The obtained ECC value is below 0.001 in the entire resonating band except at notch bands as shown in Fig. 5a. The DG and TARC for 2-unit cell MIMO design can be computed through Eqs. 2 and 3 respectively, and the calculated values for them are within acceptable limits (DG = 10 dB approx. and TARC < − 8 dB except at notch bands) as plotted in Fig. 5b,c.

$$\mathrm{DG} = 10\sqrt{(1 - \mathrm{ECC}^2)}\ (\text{In dB}) \tag{2}$$

$$\mathbf{TARC} = \sqrt{\frac{|S_{11} + S_{12}|^2 + |S_{21} + S_{22}|^2}{2}} \tag{3}$$

3.3 Design of 4-port MMSR MIMO

The layout for the 4-unit cells UWB-MIMO design is represented in Fig. 6a. The MIMO fabricated prototype with front and back views are represented in Fig. 6b and, c respectively. The inter-element isolation is improved by the orthogonal placement of elements and by providing spacing among the monopoles. In addition, it ensures miniaturization through the replacement of heavy and large decoupling or matching structures.

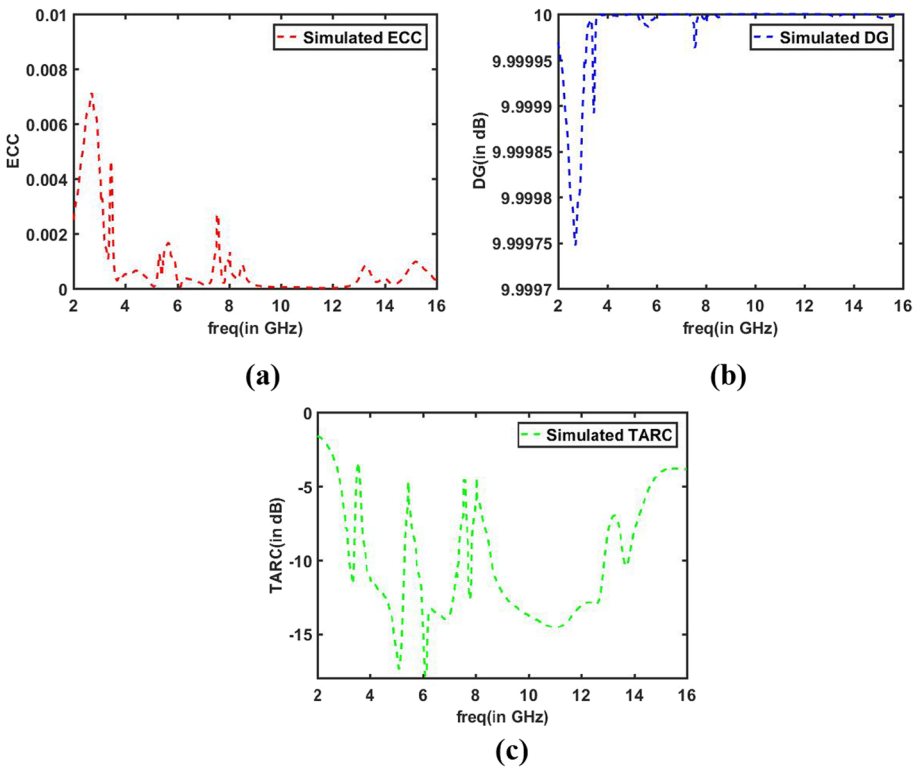

Fig. 5 Shows performance parameter analysis of 2-unit cell MIMO design **a** ECC **b** DG **c** TARC

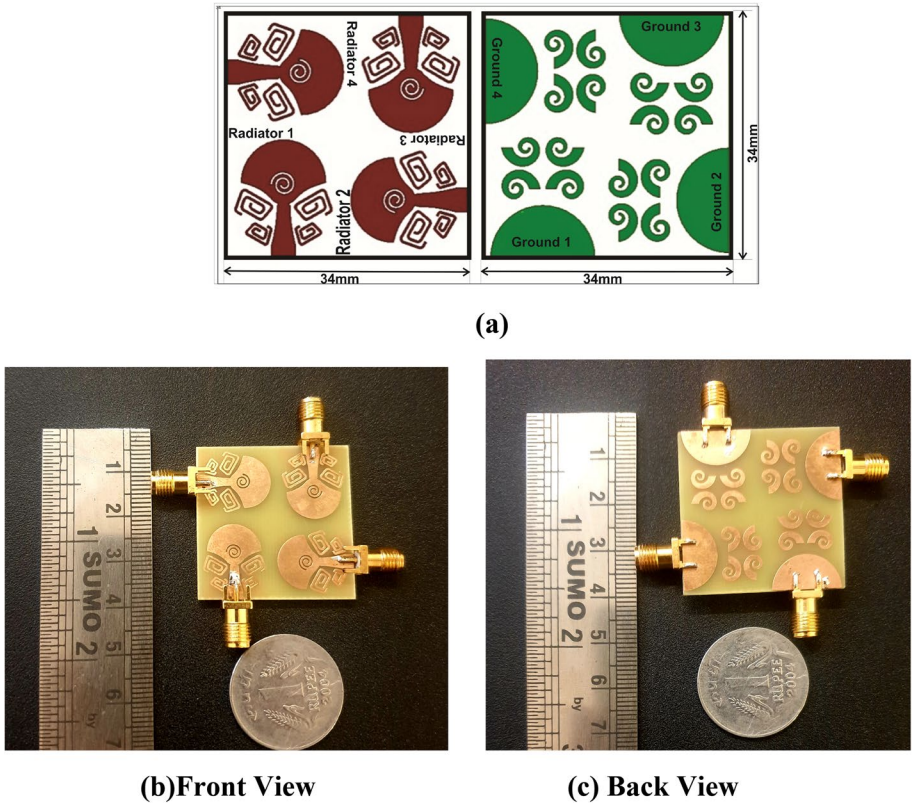

Fig. 6 Shows fabricated prototype of Four-port MIMO antenna

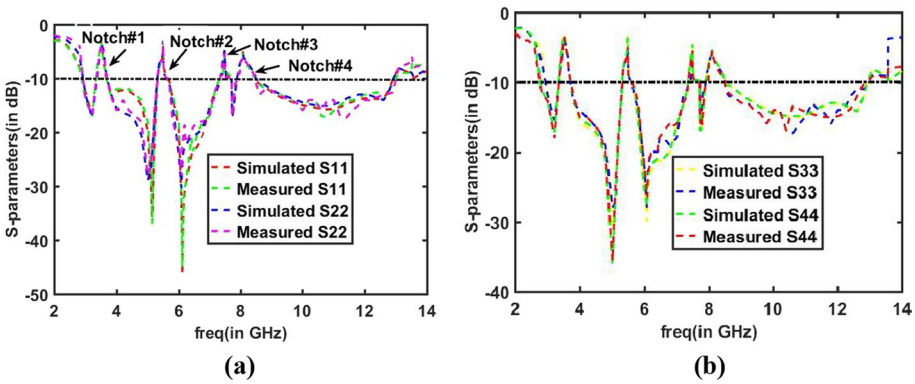

Fig. 7 Shows simulated and measured S- parameters of 4-port MIMO antenna

4 Results and discussion

The fabrication of the discussed MIMO antenna was done through the photo-etching process over the FR-4 substrate. The antenna evaluation parameters are analyzed using VNA. The SMA 50Ω connectors are used for performance measurement. The various results are analyzed in this section. In Fig. 7a, b, the various simulated and measured S-parameters representing each MIMO monopole return loss are shown. The UWB-MIMO design provides measured bandwidth of 3–12.9 GHz embedded

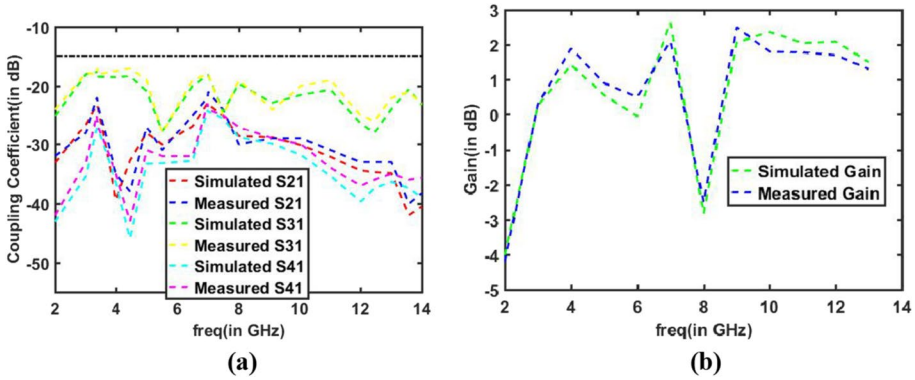

Fig. 8 Shows Four-port MIMO antenna **a** Coupling coefficients **b** Gain

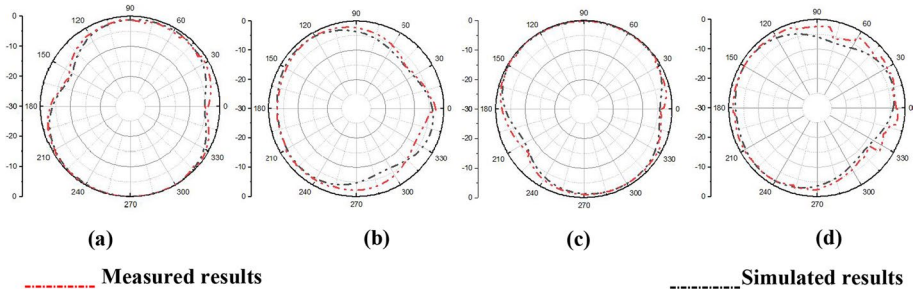

Fig. 9 Shows radiation patterns of the proposed MIMO antenna at **a** 4.5 GHz **b** 5 GHz **c** 7 GHz and **d** 9 GHz

with quad-notch behavior at 3.5 GHz (3.4–3.66 GHz), 5.5 GHz (5.3–5.61 GHz band), 7.5 GHz (7.36–7.72 GHz band) and 8.2 GHz (7.9–8.49 GHz band). The stop bands are in good agreement with the WiMAX, WLAN, satellite downlink, and satellite uplink communication bands. The notch band can be controlled by adjusting the dimensions and positions of introduced resonating structures. The Inter-coupling associated *S*-parameters are shown in Fig. 8a and it can be observed that isolation of more than 17 dB for the entire impedance bandwidth range has been achieved. In Fig. 8b, it has shown that the Gain of the antenna is 2.2 dB except at notches. The radiation pattern plot results are shown in Fig. 9. The plot is measured at port 1 while other ports are connected to matching 50Ω load. The radiation pattern is measured at 4.5 GHz, 5 GHz, 7 GHz, and 9 GHz frequencies at all ports.

The vital diversity parameters are ECC (Envelop correlation coefficient), TARC (Total active reflection coefficient), ADG (Apparent Diversity Gain), and CCL (Channel capacity loss) and for their measurement, Eqs. (4–7) are given:

For 4-port MIMO

$$\mathrm{ECC(i,j,4)} = \frac{\left|S_{i1}^{*}S_{1j} + S_{i2}^{*}S_{2j} + S_{i3}^{*}S_{3j} + S_{14}^{*}S_{4j}\right|^{2}}{\left(1 - |S_{1i}|^{2} - |S_{2i}|^{2} - |S_{3i}|^{2} - |S_{4i}|^{2}\right)\left(1 - \left|S_{1j}\right|^{2} - \left|S_{2j}\right|^{2} - \left|S_{3j}\right|^{2} - \left|S_{4j}\right|^{2}\right)} \tag{4}$$

where, $i = 1, j = 2, 3, 4$

$$DG = 10\sqrt{(1 - ECC^2)} \text{ (in dB)} \tag{5}$$

$$TARC = \sqrt{\frac{|S_{11} + S_{12} + S_{13} + S_{14}|^2 + |S_{21} + S_{22} + S_{23} + S_{24}|^2 + |S_{31} + S_{32} + S_{33} + S_{34}|^2 + |S_{41} + S_{42} + S_{43} + S_{44}|^2}{4}} \tag{6}$$

$$C = -\log_2|\psi| \tag{7}$$

where, $\psi = \begin{bmatrix} \rho_{11} & \cdots & \rho_{14} \\ \vdots & \ddots & \vdots \\ \rho_{41} & \cdots & \rho_{44} \end{bmatrix}$ $\rho_{ii} = 1 - \left|\sum_{n=1}^{4} S_{in}^* S_{ni}\right|, \rho_{ij} = 1 - \left|\sum_{n=1}^{4} S_{in}^* S_{nj}\right|$

For the 4-port UWB MIMO antenna, the acceptable values for ECC ≤ 0.3, DG ≥ 9.53 dB, TARC < 0 dB, and CCL < 0.4bits/s/Hz. It can be observed from Fig. 10a, b that, ECC (< 0.016, very less) and DG (> 9.92 dB) for the designed structure confirmed the diversity performance. The results for ECC and DG have very little variation. It is shown in Fig. 9c that TARC < -6 dB for the whole operating bandwidth. The channel capacity loss obtained is less than 0.1bits/s/Hz except for stop bands.

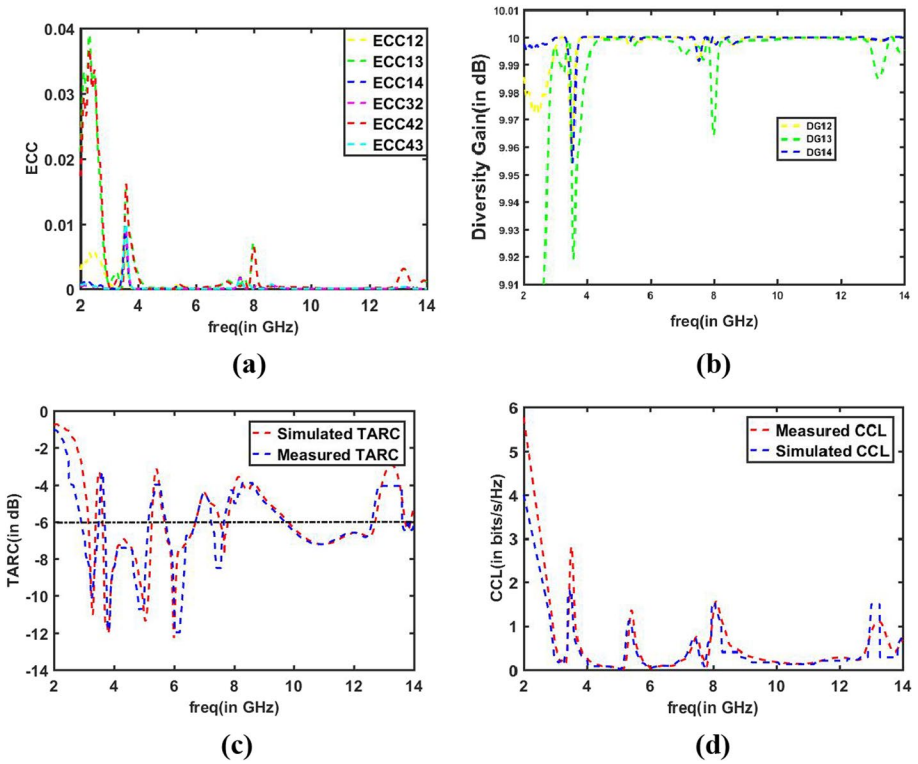

Fig. 10 Shows MIMO antenna radiation performance parameters **a** ECC **b** DG **c** TARC **d** CCL

5 Conclusion

A very small, four-port UWB-MIMO antenna with polarization diversity is reported in this article. The proposed antenna may be the best option for contemporary UWB-based MIMO applications when the performance characteristics for MIMO antennas including isolation, ECC, ADG, TARC, and channel capacity have been calculated and confirmed. Four notches are included in the proposed tapered microstrip line-fed antenna to counteract interference at licensed existing bands without sacrificing isolation, radiation performance, size, or MIMO performance. The claimed notches have a narrow band and are reasonably sharp. A slight discrepancy in the results could be attributed to cable losses, soldering problems, or fabrication tolerances. The cheap MIMO/diversity antenna construction that has been developed could be a potential source for many wireless communication systems.

Abbreviations

ECC	Envelop correlation coefficient
ADG	Apparent diversity gain
MIMO	Multiple input multiple output
TARC	Total active reflection coefficient
UWB	Ultra wideband

Author contributions

Author contributed to the study conception and design. Data Preparation, data collection and analysis were performed by Dr. Preeti Pannu. The fabrication and testing was also performed by author. Author read and approved the final manuscript.

Funding

No funding was received for this work.

Data availability

This work was performed using CST tool. So, no data available, only simulation files.

Declarations

Competing interests

Authors declare they have no financial interests.

Received: 20 November 2023 Accepted: 7 May 2024
Published online: 17 June 2024

References

1. J. Tao, Q.Y. Feng, Compact isolation-enhanced UWB MIMO antenna with band-notch character. J. Electromagn. WavEs Appl. **30**(16), 2206–2214 (2016)
2. P. Pannu, M.K. Pandey, A small square monopole ultra-wide band antenna with band stop behavior. Int. J. Eng. Technol. **7**(3.12), 697–700 (2018)
3. G. Srivastava, B.K. Kanuijia, Compact dual band-notched UWB MIMO antenna with shared radiator. Microw. Opt. Technol. Lett. **57**(12), 2886–2891 (2015)
4. Federal Communications Commission (2002) First report and order: revision of part 15 of the commission's rules regarding ultra-wideband transmission systems. ET Docket 98–153
5. S. Doddipalli, A. Kothari, Compact UWB antenna with integrated triple notch bands for WBAN applications. IEEE Access **7**, 183–190 (2018)
6. H.A. Atallah, A.B. Abdel-Rahman, K. Yoshitomi, R.K. Pokharel, CPW-Fed UWB antenna with sharp and high rejection multiple notched bands using stub loaded meander line resonator. AEU-Int. J. Electron. Commun. **83**, 22–31 (2018)
7. W. Li, Y. Hei, P.M. Grubb, X. Shi, R.T. Chen, Compact inkjet-printed flexible MIMO antenna for UWB applications. IEEE Access **6**, 50290–50298 (2018)
8. J. Ren, W. Hu, Y. Yin, R. Fan, Compact printed MIMO antenna for UWB applications. IEEE Antennas Wirel. Propag. Lett. **13**, 1517–1520 (2014)
9. R. Mathur, S. Dwari, Compact CPW-Fed ultrawideband MIMO antenna using hexagonal ring monopole antenna elements. AEU-Int. J. Electron. Commun. **93**, 1–6 (2018)
10. L. Kang, H. Li, X. Wang, X. Shi, Compact offset microstrip-fed MIMO antenna for band-notched UWB applications. IEEE Antennas Wirel. Propag. Lett. **14**, 1754–1757 (2015)

11. B.P. Chacko, G. Augustin, T.A. Denidni, Uniplanar polarisation diversity antenna for ultra-wideband systems. IET Microwaves Antennas Propag. **7**(10), 851–857 (2013)
12. Y. Zhao, F.S. Zhang, L.X. Cao, D.H. Li, A compact dual band-notched MIMO diversity antenna for UWB wireless applications. Progress Electromagn. Res. C **89**, 161–169 (2019)
13. N. Jaglan, S.D. Gupta, E. Thakur, D. Kumar, B.K. Kanaujia, S. Srivastava, Triple band notched mushroom and uniplanar EBG structures based UWB MIMO/Diversity antenna with enhanced wide band isolation. AEU-Int. J. Electron. Commun. **90**, 36–44 (2018)
14. S.P. Biswal, S. Das, A low-profile dual port UWB-MIMO/diversity antenna with band rejection ability. Int. J. RF Microwave Comput. Aided Eng. **28**(1), e21159 (2018)
15. W.A. Ali, A.A. Ibrahim, A compact double-sided MIMO antenna with an improved isolation for UWB applications. AEU-Int. J. Electron. Commun. **82**, 7–13 (2017)
16. F. Amin, R. Saleem, A compact quad-element UWB-MIMO antenna system with parasitic decoupling mechanism. MDPI Appl. Sci. **9**, 1–13 (2019)
17. Z. Wani, D. Kumar, A compact 4× 4 MIMO antenna for UWB applications. Microw. Opt. Technol. Lett. **58**(6), 1433–1436 (2016)
18. K. Srivastava, A. Kumar, B.K. Kanaujia, S. Dwari, S. Kumar, A CPW-fed UWB MIMO antenna with integrated GSM band and dual band notches. Int. J. RF Microwave Comput. Aided Eng. **29**(1), e21433 (2019)
19. D.K. Raheja, B.K. Kanaujia, S. Kumar, Compact four-port MIMO antenna on slotted-edge substrate with dual-band rejection characteristics. Int. J. RF Microwave Comput. Aided Eng. **29**(7), e21756 (2019)
20. S. Tripathi, A. Mohan, S. Yadav, A compact Koch fractal UWB MIMO antenna with WLAN band-rejection. IEEE Antennas Wirel. Propag. Lett. **14**, 1565–1568 (2015)
21. M.S. Khan, A.D. Capobianco, S. Asif, A. Iftikhar, B. Ijaz, B.D. Braaten, Compact 4× 4 UWB-MIMO antenna with WLAN band rejected operation. Electron. Lett. **51**(14), 1048–1050 (2015)
22. J. Zhu, S. Li, B. Feng, L. Deng, S. Yin, Compact dual-polarized UWB quasi-self-complementary MIMO/diversity antenna with band-rejection capability. IEEE Antennas Wirel. Propag. Lett. **15**, 905–908 (2015)
23. M.V. Berry, Z.V. Lewis, J.F. Nye, On the Weierstrass–Mandelbrot fractal function. Proc. R. Soc. London Math. Phys. Sci. **370**(1743), 459–484 (1980)
24. E. Guariglia, Entropy and fractal antennas. Entropy **18**(3), 84 (2016)
25. L. Yang, H. Su, C. Zhong, Z. Meng, H. Luo, X. Li, Y. Lu, Hyperspectral image classification using wavelet transform-based smooth ordering. Int. J. Wavelets, Multiresolut. Inform. Process. **17**(06), 1950050 (2019)
26. E. Guariglia, & S. Silvestrov (2016) Fractional-wavelet analysis of positive definite distributions and wavelets on D′(C) D′(C). in Engineering mathematics II: Algebraic, stochastic and analysis structures for networks, data classification and optimization (pp. 337–353). Springer International Publishing
27. K.C. Hwang, A modified Sierpinski fractal antenna for multiband application. IEEE Antennas Wirel. Propag. Lett. **6**, 357–360 (2007)
28. E. Guariglia, Harmonic Sierpinski gasket and applications. Entropy **20**(9), 714 (2018)

Publisher's Note